

Coupled Magnetic Excitations in Single Crystal $\text{PrBa}_2\text{Cu}_3\text{O}_{6.2}$

S.J.S. Lister¹, A.T. Boothroyd¹, N. H. Andersen², B. H. Larsen², A. A. Zhokhov³, A. N. Christensen⁴, A. R. Wildes⁵

¹ *Department of Physics, Oxford University, Clarendon Laboratory, Parks Road, Oxford, OX1 3PU, United Kingdom*

² *Risø National Laboratory, DK-4000 Roskilde, Denmark*

³ *Russian Academy of Sciences, Institute of Solid State Physics, Chernogoluka 14232, Russia*

⁴ *University of Århus, Nordre Ringgade 1, DK-8000 Århus C, Denmark*

⁵ *Insitut Laue-Langevin, B.P. 156-38042 Grenoble Cedex 9, France*

(November 2, 2018)

The dispersion of the low-energy magnetic excitations of the Pr sublattice in $\text{PrBa}_2\text{Cu}_3\text{O}_{6.2}$ is determined by inelastic neutron scattering measurements on a single crystal. The dispersion, which shows the effect of interactions with the Cu spin-waves, is well described by a model of the coupled Cu–Pr magnetic system. This enables values for the principal exchange constants to be determined, which suggest that both Pr–Pr and Cu–Pr interactions are important in producing the anomalously high ordering temperature of the Pr sublattice. Measurements of the Cu optic spin wave mode show that the inter-layer Cu–Cu exchange is significantly lower than in $\text{YBa}_2\text{Cu}_3\text{O}_{6.2}$.

PACS numbers: 71.28.+d, 74.72.Jt, 75.10.Dg, 78.70.Nx

The anomalous properties of non-superconducting $\text{PrBa}_2\text{Cu}_3\text{O}_{6+x}$ (PrBCO) [1] remain an outstanding problem in the field of cuprate superconductivity. Its magnetic properties are strikingly different from those of other members of the RBCO family (where R is a rare earth, Y or La). Long range antiferromagnetic order in both the Cu and Pr sublattices along with semiconducting resistivity persist over the entire range of oxygen doping $0 < x < 1$, and the magnetic transition in the Pr sublattice occurs at a temperature T_{Pr} an order of magnitude higher than for other rare earths in RBCO [2]. It is now generally believed that these anomalous properties are caused by a hybridisation of the Pr $4f$ and O $2p$ orbitals. In particular, an influential model of the electronic structure of PrBCO [3] explains the absence of superconductivity by a localisation of the holes in hybridised Pr–O bonds. Given the likelihood that the electronic and magnetic properties of PrBCO, including the occurrence of superconductivity [4], both depend on this hybridisation, detailed information on the strengths and symmetries of the magnetic interactions is desirable.

In this Letter, we describe inelastic neutron scattering measurements of the magnetic excitations of PrBCO made for the first time on a single crystal. Using this data and a spin wave model of the coupled Cu–Pr system we have independently determined the magnitudes of the Pr–Pr, Cu–Pr and Cu–Cu interactions. We find that the Pr–Pr interaction is unexpectedly strong and would alone lead to T_{Pr} being substantially higher than the rare-earth ordering temperature in other RBCO. We have also identified the effects of a pseudo-dipolar component to the Cu–Pr coupling on the magnetic excitations. Finally, we show that the inter-layer Cu–Cu exchange is reduced by a factor of two in PrBCO relative to YBCO.

The experiments were performed on a crystal of $\text{PrBa}_2\text{Cu}_3\text{O}_{6.2}$ of mass 2g prepared by top seeding a flux. The crystal mosaic was $\sim 1^\circ$ and $T_{\text{Pr}} = 13\text{K}$. Measurements on the triple-axis spectrometers TAS 6 at

Risø and IN8 at the ILL were made at energy transfers up to 10 meV and 70 meV respectively. A horizontally-focussing analyser was employed to increase the measured signal at the expense of some resolution in the scattering vector \mathbf{Q} . The crystal was mounted in a ^4He cryostat and measurements were made in the $(h, k, 0)$ or (h, h, l) scattering planes.

Previous neutron scattering measurements on polycrystalline samples of PrBCO_6 revealed two peaks centred at 1.7 and 3.4 meV at $T = 5\text{K}$, which shifted to lower energies as T_{Pr} was approached [5]. These peaks correspond to excitations of the Pr ions subject to the local exchange and crystal fields. To investigate the \mathbf{Q} dependence of these excitations we performed energy scans at $T = 1.8\text{K}$ at points in reciprocal space primarily along the principal symmetry directions of the magnetic zone. Fig. 1 shows representative scans at $\mathbf{Q} = (0, 0, 2.2)$ and $(0.75, 0.75, 0)$. Two peaks, labelled A and B, are observed at energies consistent with the polycrystalline data. Fig. 1 also illustrates the variation in intensity of the excitations with the direction of \mathbf{Q} . The intensity of peak A is largest when \mathbf{Q} is in the ab plane, and is reduced for $\mathbf{Q} \parallel \mathbf{c}$. Peak B exhibits the opposite trend. The width of both peaks (1-2 meV FWHM) is larger than the energy resolution of the spectrometer (0.4 meV FWHM). The implied intrinsic broadening is consistent with relaxation due to hybridisation as suggested earlier from the spectrum of polycrystalline PrBCO [5]. The use of a single crystal, however, shows that the observed broadening is not solely due to dispersion.

Single crystals also enable us to study the dispersion of the excitations, which is a central objective of this work. The insets to Fig. 1 show the low-energy data corrected for the non-magnetic background and elastic peak measured on a similar-sized crystal of $\text{YBCO}_{6.2}$. The line shows a function comprising two damped harmonic oscillator response functions (including detailed balance factor) fitted to the data. No variation in the energy of peak

B was apparent to within the experimental uncertainty. The energy dispersion of peak A was obtained by fitting a single response function to the data for $E \leq 3$ meV. The results are shown in Fig. 2. A number of scans were also made at $\mathbf{Q} = (h, h, l)$ for $l \neq 0$, but no measurable dispersion along the c -axis was observed.

We also studied the excitations of the Cu sublattice. The Cu spin waves in antiferromagnetic YBCO have been described by Tranquada *et al.* [6]. Due to the bilayer structure of YBCO the spectrum consists of two acoustic and two optic modes, each pair being split into in- and out-of-plane modes by the anisotropy (a few meV in YBCO). The optic mode is of interest because its energy depends on the exchange coupling between adjacent layers, which could be sensitive to the electronic structure of the Pr ion. To measure the optic mode at the magnetic zone centre a number of constant energy scans were made in the $(h, h, 0)$ direction through the point $(\frac{1}{2}, \frac{1}{2}, 6.75)$, close to where the optic mode has maximum intensity. Scans at 45 and 55 meV are shown in Fig. 3(a). All scans at energies above ~ 50 meV have a peak centred at $h = \frac{1}{2}$, which we interpret as being due to the optic mode. The amplitude of this peak exhibits a stepwise increase with energy, as shown in Fig. 3(b). The optic mode gap, taken from the mid-point of the step, is 53 ± 2 meV. The corresponding energy for YBCO_{6.2} estimated in the same way from the available data [7] is 70 ± 5 meV.

We now consider a model to describe the dispersion of peak A. The model is based on the single-ion states of Pr³⁺ in the tetragonal crystalline electric field (CEF). We obtained these states by refining a model for the CEF using the observed energy spectra of polycrystalline PrBCO₆ [8]. The refinement gave a doublet ground state with a first excited state a few meV higher in energy, consistent with previous analyses [5,8]. To take into account the magnetic ordering at $T < T_{\text{Pr}}$ we included a molecular field. This field lifts the degeneracy of the ground-state doublet, hence we interpret peak A in Fig. 1 as the transition within the exchange-field-split doublet. Peak B is then the transition from the ground state to the crystal field singlet. We chose the magnitude and direction of the molecular field to reproduce the average energy of peak A and the observed direction of the moment [9] at about 45° to the c axis [10]. The observed variation of the relative intensity of peaks A and B with the direction of \mathbf{Q} is consistent with the cross-sections calculated from the CEF wavefunctions.

The simplest model for the dispersion of peak A is then given by the Hamiltonian:

$$H_{\text{Pr}} = H_{\text{CEF}} + \frac{1}{2} J_{\text{Pr}} \sum_{\langle ij \rangle} (\mathbf{J}_i - \langle \mathbf{J}_i \rangle) \cdot (\mathbf{J}_j - \langle \mathbf{J}_j \rangle) \quad (1)$$

where J_{Pr} represents an isotropic exchange interaction between nearest-neighbour Pr ions (assumed to be > 0

consistent with the observed antiferromagnetic ordering of the Pr moments), \mathbf{J}_i is the angular momentum of a Pr ion and H_{CEF} is the single-ion crystal field Hamiltonian including the molecular-field term. The summation in (1) is over all pairs of nearest-neighbouring Pr ions. We use the pseudo-boson approximation [11] to calculate the dispersion from (1). This method gives a simple relation between matrix elements of the calculated crystal field states and operators corresponding to deviations of the angular momentum from the mean-field values. Here we only include the transition within the doublet ground state, as the exchange coupling does not give appreciable mixing with the singlet level. The resulting dispersion of the doublet transition has two branches (due to the antiferromagnetic order) whose degeneracy is lifted by the non-zero x component of the exchange field. In practice, only one of the two modes is actually observed at a given \mathbf{Q} owing to the variation in intensity between magnetic zones. The higher energy mode has a much larger cross-section near magnetic reciprocal lattice vectors that coincide with nuclear Bragg reflections (e.g. $(1, 1, 0)$) whereas the lower energy mode has maximum intensity at the reciprocal lattice points corresponding to magnetic-only reflections (e.g. $(\frac{1}{2}, \frac{1}{2}, 0)$). This intensity variation is in agreement with that observed experimentally, providing further confirmation for the identification of peak A with the intra-doublet transition, and for the assumption of an exchange field at an angle to the c axis.

As a first approximation, we then attempt to fit this dispersion relation to the experimental data by varying J_{Pr} . The best fit is given by $J_{\text{Pr}} = 0.029$ meV, and is shown by the broken line in Fig. 2. Although the general form of the dispersion is reasonably well described by this model involving only the Pr sublattice, there is clear evidence of a discrepancy near the magnetic zone centre. This deviation suggests that we need to consider the effect of interactions between the Pr excitations and the spin-wave excitations of the Cu sublattice. Owing to the very high Cu spin-wave velocity, these interactions are only important close to the magnetic zone centres at low energies. We model the Cu-Pr coupling with the same anisotropic term that has been found necessary to explain the observed non-collinear magnetic structure [9,12,13].

$$H_{\text{Cu-Pr}} = \frac{1}{2} \sum_{\alpha\beta, \langle ij \rangle} K_{\alpha\beta}(ij) S_{\alpha i} J_{\beta j} \quad (2)$$

where α, β label components $\{x, y, z\}$, $\mathbf{K}(ij)$ is a tensor describing the pseudo-dipolar interaction (consistent with the tetragonal symmetry of the crystal), and \mathbf{S} denotes the spin of a Cu ion. A similar term was also used to describe the excitations in Nd₂CuO₄ [14].

For the interactions between Cu spins (H_{Cu}), we employ the model used to describe the spin excitations of antiferromagnetic YBCO [6]. This incorporates nearest-neighbour couplings in-plane J_{\parallel} and between planes J_{\perp} ,

and an out-of-plane anisotropy. The optic mode gap at the zone centre is $2\sqrt{J_{\parallel}J_{\perp}}$. For YBCO_{6.2} the value of J_{\parallel} , determined by Hayden *et al* [7], is 125 ± 5 meV. Here, we use a value of $J_{\parallel} = 127 \pm 10$ meV recently obtained on our crystal of PrBCO_{6.2} by inelastic neutron scattering [16], consistent with Raman data [15]. Combined with our measurement of the optic gap, this value of J_{\parallel} leads to $J_{\perp} = 5.5 \pm 0.9$ meV. We note the surprising result that the value of J_{\perp} for PrBCO_{6.2} is a factor of 2 lower than that for YBCO_{6.2} ($J_{\perp} = 11.5 \pm 1.5$ [7]).

Above T_{Pr} the Cu ordering is similar to that observed in YBCO₆, however the presence of the interaction given by (2) leads to a modification of the Cu magnetic structure at temperatures below T_{Pr} . The magnetic moments on neighbouring Cu planes are observed to counter-rotate about the c axis by an angle ϕ [9,17]. This twist can be accounted for in our model by minimising the contribution to the ground state energy from the J_{\perp} and pseudo-dipolar terms. The result is

$$\sin \phi = 8\langle J_x \rangle \langle S \rangle K_{xy} / J_{\perp} \quad (3)$$

where J_x is the x -component of the Pr angular momentum. The more general problem of verifying that the observed magnetic structure minimises the energy of the combined Cu-Pr system has been considered in [12].

Having modified H_{Cu} to take into account this ground state configuration, the excitation spectrum of the complete Hamiltonian $H = H_{\text{Cu}} + H_{\text{Pr}} + H_{\text{Cu-Pr}}$ is obtained from the bilinear terms in the spin-deviation operator expansion in the usual way. As a result of the pseudo-dipolar Cu-Pr interaction the spectrum is modified in two ways. First, the bilayer twist ϕ leads to a gap in the in-plane acoustic Cu mode (the out-of-plane mode is also raised and continues to lie a few meV higher). Measurements below T_{Pr} at higher energies indicate that the gap is $\simeq 10$ meV. Secondly, the two Pr excitation branches are both significantly affected at the magnetic zone centre by coupling with the Cu modes [18]. As would be expected, the Pr spectrum is little affected away from the zone centres because of the steepness of Cu spin-wave branch.

Of the four independent components of the tensor \mathbf{K} , the major contribution at the zone centre is from K_{xy} . The other components produce only relatively small effects, not varying very strongly with \mathbf{Q} . Given that the Pr-Pr interaction can account for the dispersion away from the zone centre satisfactorily, we next fit the data with the dispersion of the full model by varying the parameters J_{Pr} and K_{xy} . A good agreement is obtained, as shown by the solid line in Fig. 2 which corresponds to the values $J_{\text{Pr}} = 0.025$ meV and $K_{xy} = 0.30$ meV (the statistical errors in the fitted parameters are better than 10%), although near the nuclear zone centre the predicted dispersion is so steep that the limited resolution of the spectrometer will limit the extent to which the model can be tested. Further support for the fitted value of K_{xy} comes

from (3) which, together with $\langle S \rangle = 1/2$ and $\langle J_x \rangle = 1.9$ from the single-ion model, gives $\phi = 22^\circ$, in good agreement with the observed value of $\phi = 20 \pm 5^\circ$ [9]. However, we should also mention two remaining shortcomings of the model. First, the fitted values for the exchange constants only produce a molecular field at the Pr site about half the size of that required to produce the observed energy splitting. Secondly, the crystal field model predicts a Pr moment of $2\mu_B$ compared to the measured value of $1.2\mu_B$. These discrepancies may indicate that the electronic state of the Pr ion is not completely accounted for by the crystal field model, and that other effects such as covalency need to be considered.

Before concluding, we consider the magnitude of K_{xy} and J_{Pr} in comparison with other related measurements. Although no previous attempts have been made to determine the Cu-R coupling in RBCO compounds, a similar pseudo-dipolar term seems to be present in Nd₂CuO₄, for which a value of $K_{xy} = 0.075$ meV was found, a factor 4 less than found here for PrBCO [14]. As for the size of J_{Pr} , we can judge this by making a simple estimate from mean-field theory of T_{Pr} assuming J_{Pr} to be the only interaction present. This requires a calculation of the single ion susceptibility using the same crystal field parameters as previously and predicts $T_{\text{Pr}} \approx 7$ K. This value is surprisingly large, suggesting that the high value of T_{Pr} observed experimentally is due not only to a significant Cu-Pr interaction but also to large value of the Pr-Pr exchange.

The central result of the work described in this paper is the set of exchange constants K_{xy} , J_{Pr} and J_{\perp} , determined for PrBCO for the first time. These three constants are important because they reflect exchange pathways that depend on Pr $4f$ states, and so contain information on the underlying electronic structure of PrBCO. The J_{Pr} , K_{xy} are found to be surprisingly large, and this shows that both the Pr-Pr and Cu-Pr interactions are relatively strong in comparison to the corresponding interactions in other cuprates. J_{\perp} , on the other hand, is found to be a factor of two smaller in PrBCO than in YBCO, indicating that Pr has a significant influence on the interlayer exchange coupling. These results provide insight into the anomalous electronic and magnetic properties of PrBCO, and suggest that the calculation of exchange interactions in PrBCO could be a very valuable test of models for its electronic structure. Similar experiments on an oxidised crystal of PrBCO, for which the effects of hybridisation could be even more pronounced, are planned for the near future.

We acknowledge the financial support of the EPSRC, and the EU TMR Programme enabling the experiments to be performed at Risø.

- [1] H. B. Radousky, J. Mater. Res. **7**, 1917 (1992).
- [2] P. M. Allenspach and M. B. Maple, in *Handbook on the Physics and Chemistry of Rare Earths*, edited by K.A. Gschneidner Jr., L. Eyring, M. B. Maple, (North-Holland, Amsterdam, in press), Vol. 31; A. T. Boothroyd, J. Alloys and Compounds **303-304**, 489 (2000).
- [3] R. Fehrenbacher and T. M. Rice, Phys. Rev. Lett. **70**, 3471 (1993).
- [4] Z. Zou *et al.*, Jpn. J. Appl. Phys. Lett. **36**, L18 (1997).
- [5] H.-D. Jostarndt *et al.*, Phys. Rev. B **46**, 14872 (1992).
- [6] J. M. Tranquada *et al.*, Phys. Rev. B **40**, 4503 (1989).
- [7] D. Reznik *et al.*, Phys. Rev. B **53**, R14741 (1996); S. M. Hayden *et al.*, Phys. Rev. B **54**, R6905 (1996). These authors find $J_{\perp} = 9-10$ and 11 ± 2 meV respectively. Our measurements on YBCO_{6.2} give $J_{\perp} = 13 \pm 2$ meV.
- [8] G. Hilscher *et al.*, Phys. Rev. B **49**, 535 (1994).
- [9] A. T. Boothroyd *et al.*, Phys. Rev. Lett. **78**, 130 (1997).
- [10] The orthogonal axes x, y, z are defined here with x in the ab plane of the crystal parallel to the in-plane direction of the Pr moment, and z along the c axis.
- [11] T. M. Holden and W. J. L. Buyers, Phys. Rev. B **9**, 3797 (1974).
- [12] S. V. Maleev, JETP Lett. **67**, 947 (1998)
- [13] A. T. Boothroyd, Physica B **241-243**, 792 (1998)
- [14] R. Sachidanandam *et al.*, Phys. Rev. B **56**, 260 (1997).
- [15] M. Yoshida, N. Koshizuka and S. Tanaka, Phys. Rev. B **42**, 8760 (1990)
- [16] S. J. S. Lister *et al.*, unpublished.
- [17] X-ray scattering studies have also revealed a small incommensurate component in the Pr magnetic structure with wave vector $(1/2 \pm \delta, 1/2, 0)$, but the period corresponding to δ is sufficiently large for a significant effect on the excitations to be unlikely. J.P. Hill *et al.*, Phys. Rev. B **61**, 1251 (2000).
- [18] From the structure of the eigenfunctions of the excitations, it appears that the K_{xy} component of the tensor couples the Cu in-plane acoustic branch with the higher energy Pr excitation, and the in-plane optic mode to the lower energy Pr excitation. Since the out-of-plane modes do not couple to the Pr excitations, the value of the out-of-plane anisotropy is not crucial here, so we take the same value as found for YBCO.

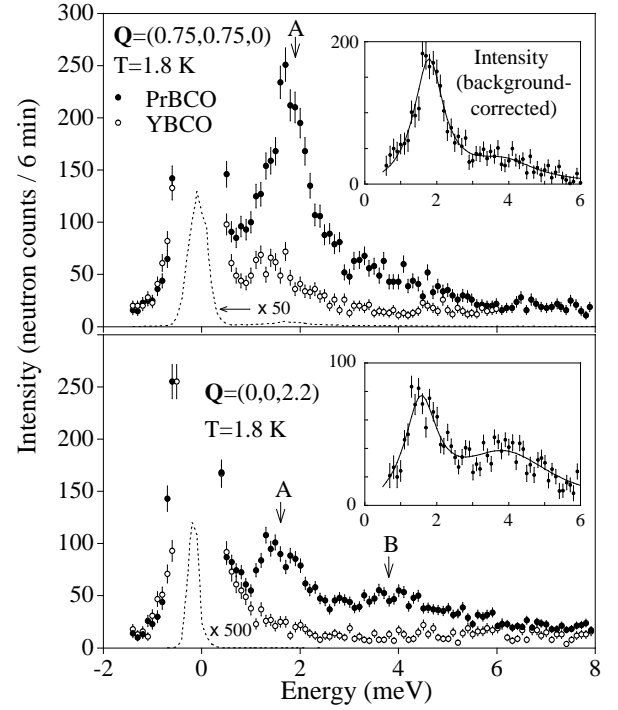


FIG. 1. Neutron inelastic scattering from PrBCO and YBCO at 1.8 K, for $\mathbf{Q}=(0, 0, 2.2)$ and $(0.75, 0.75, 0)$. The elastic peak from PrBCO is shown by the broken curve (reduced by a factor of 50). Fits to the PrBCO data corrected with the YBCO as a non-magnetic background is shown in the insets.

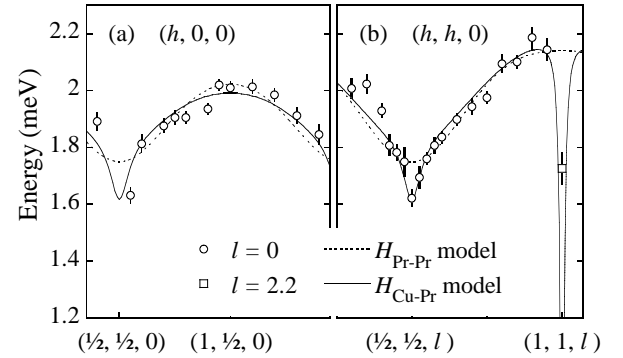


FIG. 2. Dispersion of the low-energy Pr excitation. The measured data, obtained by fitting as shown in Fig. 1, are plotted with open symbols. The error bars are the standard deviations from the fitting procedure, but in some cases the points are the result of averaging several runs and the errors are then correspondingly reduced. The broken line is a fit to a model for the Pr sublattice only, while the solid line is a fit to the full model including a Cu-Pr interaction. $(0.5, 0.5, 0)$ and $(1, 1, 0)$ correspond to the centre of adjacent magnetic zones, so that the zone boundary is crossed at $(0.75, 0.75, 0)$, but only the low energy mode has a measurable intensity in the first zone, and the high-energy mode in the second.

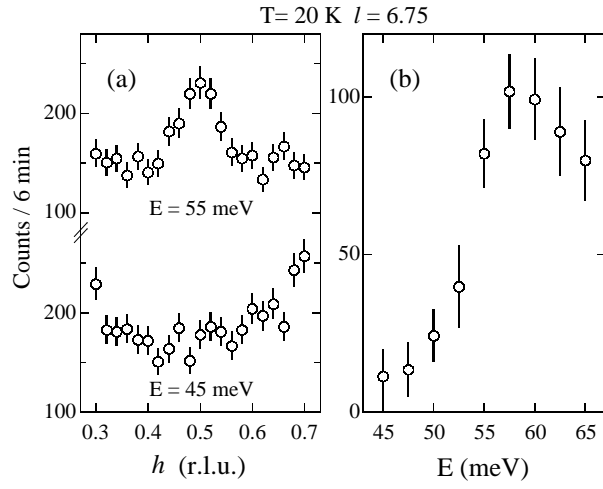


FIG. 3. (a) Measurement of the optic spin wave in PrBCO by neutron inelastic scattering. Constant energy scans at 45 and 55 meV through $(0.5, 0.5, 6.75)$ parallel to $(h, h, 0)$ (in reciprocal lattice units (r.l.u.)) are shown. (b) The amplitude of the observed peaks as a function of energy transfer.